CATALYSIS, KINETICS AND REACTORS
Chinese Journal of Chemical Engineering, **17**(3) 394—400 (2009)

Quantum Chemistry Studies on the Free-radical Growth Mechanism of Polycyclic Arenes from Benzene Precursors*

ZHANG Riguang (章日光)[1], **WANG Baojun** (王宝俊)[1,**], **TIAN Yajun** (田亚峻)[2] **and LING Lixia** (凌丽霞)[1]
[1] Key Laboratory of Coal Science and Technology (Taiyuan University of Technology), Ministry of Education and Shanxi Province, Taiyuan 030024, China
[2] Key Laboratory of Multiphase Reactions, Institute of Process Engineering, Chinese Academy of Sciences, Beijing 100190, China

Abstract The free-radical growth mechanisms for the formation of polycyclic arenes (PCAs) were constructed based on the block unit of benzene, and were calculated by the quantum chemistry PM3 method. Two kinds of reaction paths are proposed and discussed. The calculation results show that the formation of PCAs is only controlled by the elimination of H atom from benzene, and the corresponding activation energy is 307.60 kJ·mol^{-1}. H_2 is only the effluent gas in our proposed reaction mechanism, and the calculation results are in accord with the experimental facts.
Keywords benzene, polycyclic arene, mechanism, quantum chemistry calculation

1 INTRODUCTION

Carbon nanotubes (CNTs) are becoming an increasingly important class of materials, and their properties and synthesis routes have been extensively studied. It has been indicated that the small arenes (such as benzene or naphthalene) are feasible materials for the production of CNTs, because their aromatic structures are quite similar to the C—C bonding characteristics of the graphene sheet of carbon nanotubes, and corresponding growth mechanisms have been presented. It was speculated that the small polycyclic arenes (PCAs) formed before the building up of the CNTs probably played a positive role in the mass production of CNTs [1−3]. Therefore, the investigation of the formation of PCAs is significant. The formation mechanisms of PCAs has been previously proposed: Frenklach and co-workers [4, 5] developed a model for the formation of PCAs, which involved the successive loss of ring hydrogen atoms followed by acetylene addition to the ring and subsequent ring closure reaction; the Bittner-Howard mechanism [6] also involved acetylene additions, but in this mechanism, the second acetylene molecule was added to the first one, which then reacted with an existing ring to form an additional ring; and the third mechanism involved the reaction of two C_5H_5 rings followed by a rearrangement to form two fused C_6 rings [7].

Recently, well-graphited and quasi-aligned CNTs have been produced with benzene [8, 9], and the thermal analysis-mass spectroscopy technique was applied to clarify the growth mechanism of CNTs. A surprising fact was that no possible hydrocarbon species derived from benzene were detected, indicating that the C—C bond was not broken under the experimental conditions. As a result, the six-member-ring growth mechanism was reasonably put forward [8]. This mechanism suggested that the PCAs were built up based on the block unit of benzene.

With the rapid development of computational chemistry in the last few years, it has been used as a powerful tool to verify researchers' guesses from a microcosmic point of view, to present clear image of many chemical processes, and to reveal the essence of various processes and phenomena [10−14]. However, few studies on the growth of PCAs according to the six-member-ring mechanism have been conducted [15].

In terms of the six-number-ring growth mechanism of CNTs proposed by our previous work [8], the kinetic models of PCAs formation without ring-opening and from benzene precursors were established in our investigation, and the growth mechanism of the whole process (including dehydrogenation, condensation and fused ring) was theoretically studied using the quantum chemistry calculation method.

2 MODEL CONSTRUCTION AND COMPUTATIONAL METHOD

According to the experimental results [8], two competitive reaction paths were designed to describe the growth mechanism of PCAs, as shown in Fig. 1. Every reaction step of the two constructed paths was interpreted in terms of the main microscopic features of bond order, Mulliken population, net charge and frontier orbital energy, *etc*. The cycle forming P1 was defined as Cycle 1, and the reaction cycle using the product of previous cycle as the reactant and following the same reaction mode was defined as Cycles 2−6, respectively.

Due to the large molecular structure discussed in

Received 2008-10-13, accepted 2009-04-17.
* Supported by the National Basic Research Program of China (2005CB221203), the National Natural Science Foundation of China (20576087, 20776093, 50534070) and the Natural Science Foundation of Shanxi Province (2006011022, 2009021015).
** To whom correspondence should be addressed. E-mail: wangbaojun@tyut.edu.cn

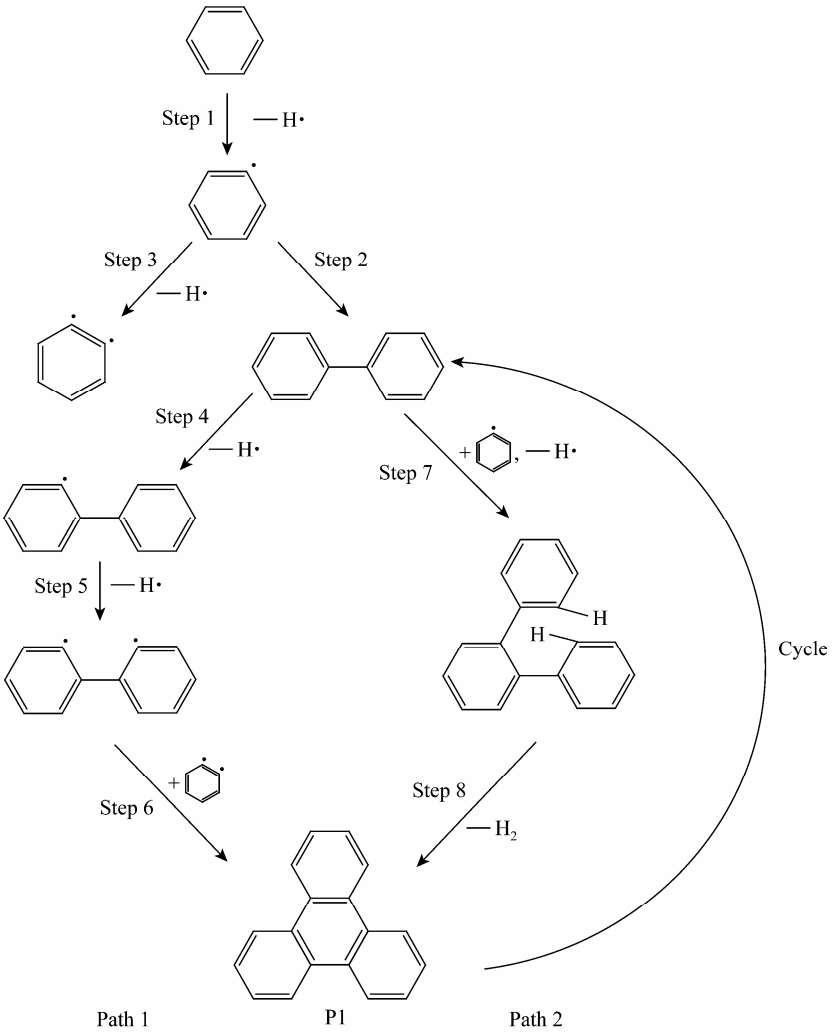

Figure 1 The Cycle 1 of reaction mechanism from benzene precursor

this research, theoretical calculations were carried out using the semi empirical PM3 method in the MOPAC 7.0 program [16]. The initial estimates of the geometry of all the structures including reactants, products, intermediates (IM) and transition states (TS) were obtained by the molecular mechanics program of CS ChemOffice Pro [17], followed by full optimization of all geometric variables (bond lengths, bond angles and dihedral angles). A lot of free-radicals were involved, so spin unrestricted was chosen. The keyword "precise" was selected because of the energy comparison of near structures. Vibrational analyses were carried out to characterize them as either equilibrium structures (all real harmonic vibrational frequencies) or transition states (one and only one imaginary vibrational mode corresponding to the reaction coordinate). Zero point vibrational energies (ZPE) were taken into account. All the calculations were carried out on a Lenovo personal computer (Lenovo Co., China) with a P4 3.2 G CPU and 1 GB internal memory.

In order to evaluate the reliability of the selected method and parameters, the bond dissociation energy (BDE) of several molecules were calculated, and the comparison of the calculation and experimental results was shown in Table 1. As we can see, the calculation results are in agreement with experimental structural parameters, the largest deviation of BDE is lower than 2.0 kJ·mol^{-1}.

Table 1 Comparison of bond dissociation energies between the calculation and experimental values

Model compound	Radical X·	H_f/kJ·mol^{-1}	BDE/kJ·mol^{-1}	
			Cal.	Exp.[18]
H—H	H·	217.995	435.990	436.002
F—F	F·	79.036	158.072	156.996
Cl—Cl	Cl·	121.294	242.588	242.580

Note: H_f denotes the heat of formation of different free-radicals.

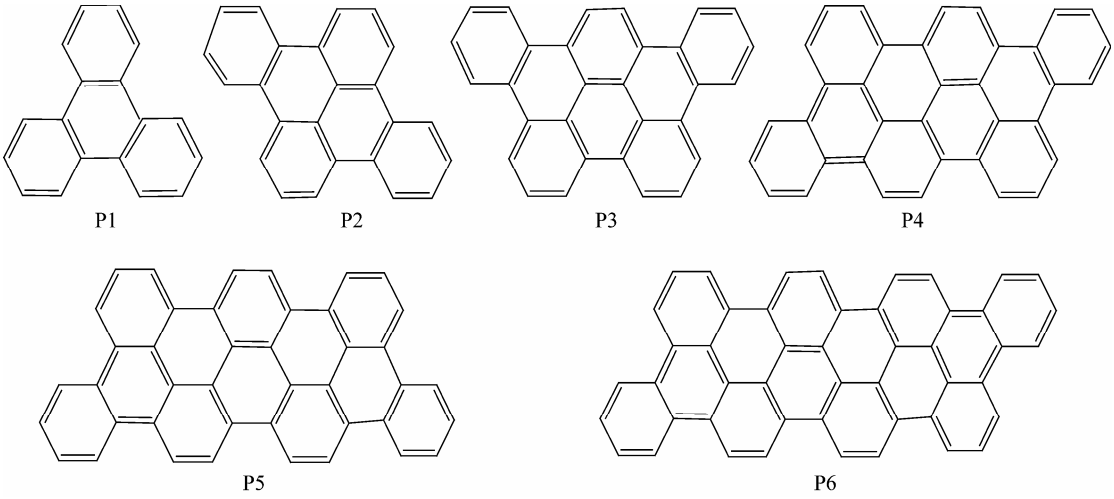

Figure 2 The produced PCAs during the growth process

3 RESULTS AND DISCUSSION

According to the transition state theory of Eyring [10], the activation energies of every step along the growth cycles of PCAs, derived from the energy difference between a transition state and a reactant or an intermediate, were calculated. Correspondingly, the produced PCAs grew step by step from P1 ($C_{18}H_{12}$) to P6 ($C_{48}H_{22}$) (shown in Fig. 2), and the growth process using benzene as a block unit without ring-opening went through six cycles.

3.1 Formation process of PCAs through Path 1

Path 1 mainly focuses on the dissociation of the C—H bond from benzene or PCAs, Steps 2 and 6 are the free-radical combination reaction without an energy barrier, in other words, the reaction activation energy is zero. Steps 1, 3, 4 and 5 are homolytic cleavage of C—H bond, and the activation energies of every step in different cycles are listed in Table 2.

Table 2 The activation energy of every step of Path 1 in different cycles

Cycle	Activation energy E_a/kJ·mol^{-1}			
	Step 1	Step 3	Step 4	Step 5
1	307.60	270.79	291.97	276.59
2	307.60	270.79	286.46	268.97
3	307.60	270.79	255.13	246.74
4	307.60	270.79	253.22	236.76
5	307.60	270.79	246.56	233.76
6	307.60	270.79	245.36	229.46

Steps 1 and 3 are the common steps for every cycle, and the corresponding activation energies keep at constant. With the growth of PCAs, it can be seen from Table 2 that the activation energies of Steps 4 and 5 gradually decrease, which could be explained by the average Mulliken population of the C—H bond in the subsequent discussion. Then, the activation energies of Steps 4 and 5 have a decreasing tendency. Therefore, Step 1 is the rate-determining step in Path 1, and the corresponding activation energy is 307.60 kJ·mol^{-1}.

3.2 Formation process of PCAs through Path 2

Obtaining specific information for the formation process of Path 2 is relatively complicated in contrast to Path 1. By searching the transition states of Path 2 in Cycle 1, it is found that Step 7 is an elementary reaction *via* one transition state TS1 leading to IM1; however, from IM1 to P1, Step 8 involves three transition states (TS2, TS3 and TS4) and two intermediates (IM2 and IM3). The typical geometry structural parameters of the transition states and intermediates are shown in Fig. 3 and Table 3. The detailed reaction process is followed by IM1→TS2→IM2→TS3→IM3→TS4→P1.

It can be seen from Table 3 that the C6-C9 distance in the process of IM1→P1 is shorten from 0.386 nm to 0.142 nm, and the process has a tendency to form a conjugate structure. At the same time, the C1—C12 and C2—C5 bond lengths decrease from 0.147 nm to 0.142 nm, gradually approaching the C—C bond length in benzene molecule. Moreover, the lengths of the C6—H14 and C9—H13 bond are much longer than that of the common C—H bond, adequately reflecting the process of H-elimination. ∠C12—C9—C6 decreases from 151.2° in IM2 to 120.0° in P1, suggesting that the reaction takes place towards the direction of the conjugate structure. In the IM2→P1 process, the ∠C12—C1—C2 and ∠C2—C5—C6 disciplinarily decrease to 120.0° for the formation of the conjugate structure. With the reaction going on, the dihedral angles of C9—C12—C1—C2 and

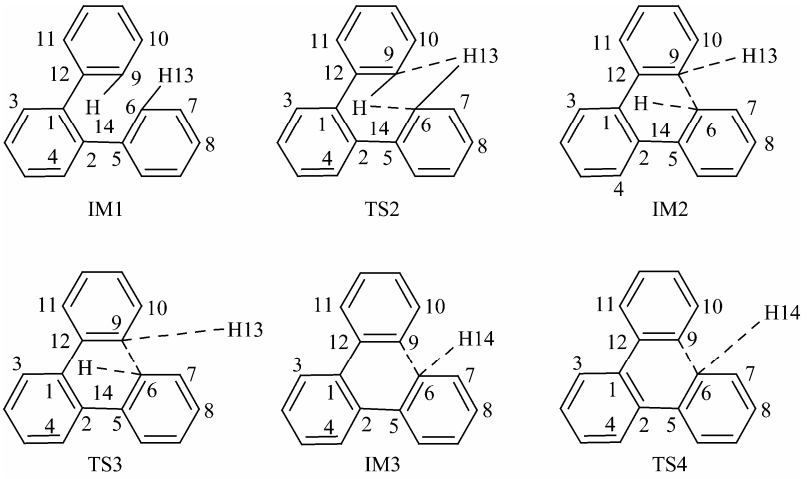

Figure 3 The atomic number of transition states and intermediates in Step 8

Table 3 The typical geometry structural parameters of transition states and intermediates in Path 2

Species	Bond length/nm		Bond angle/(°)		Dihedral angle/(°)	
IM1	C6—C9	0.386	∠C12—C9—H14	119.7	C2—C1—C12—C9	108.5
	C9—H14	0.110	∠H13—C6—C5	119.6	C1—C2—C5—C6	–61.2
	C6—H13	0.110	∠C12—C1—C2	124.4	C12—C1—C2—C5	0.0
	C1—C12	0.147	∠C2—C5—C6	123.0	H13—C6—C5—C2	–178.7
TS2	C6—C9	0.343	∠C9—H14—C6	63.4	C2—C1—C12—C9	98.4
	C9—H14	0.110	∠C9—H13—C6	78.4	C1—C2—C5—C6	–36.9
	C6—H13	0.394	∠C12—C1—C2	123.5	C12—C1—C2—C5	0.9
	C9—H13	0.110	∠C2—C5—C6	123.1	H13—C6—C5—C2	–96.1
IM2	C6—C9	0.278	∠C12—C9—C6	151.2	C2—C1—C12—C9	58.6
	C9—H13	0.240	∠H14—C6—C9	131.5	C1—C2—C5—C6	–26.7
	C6—H14	0.233	∠H13—C9—C6	134.9	C12—C9—C6—H14	66.7
	C1—C12	0.147	∠C9—C6—C5	119.9	H13—C9—C6—C7	65.8
TS3	C6—C9	0.282	∠C12—C9—C6	146.7	C2—C1—C12—C9	9.8
	C9—H13	0.440	∠H14—C6—C9	33.5	C1—C2—C5—C6	–9.2
	C6—H14	0.244	∠H13—C9—C6	81.0	H13—C9—C6—C7	8.3
	C1—C12	0.144	∠C2—C5—C6	122.3	C12—C9—C6—H14	119.4
IM3	C6—C9	0.172	∠C12—C9—C6	134.7	C2—C1—C12—C9	5.6
	C6—H14	0.240	∠H14—C6—C9	39.9	C1—C2—C5—C6	–6.7
	C1—C12	0.144	∠C12—C1—C2	121.9	C12—C9—C6—H14	96.7
	C2—C5	0.143	∠C9—C6—C5	120.9	C12—C9—C6—C5	–6.7
TS4	C6—C9	0.142	∠C12—C9—C6	121.7	C2—C1—C12—C9	2.1
	C6—H14	0.412	∠C12—C1—C2	121.1	C1—C2—C5—C6	–1.7
	C1—C12	0.142	∠C9—C6—C5	120.2	C12—C9—C6—C5	–0.7
	C2—C5	0.142	∠C2—C5—C6	120.6	C12—C9—C6—H14	16.7
P1	C6—C9	0.142	∠C12—C9—C6	120.0	C2—C1—C12—C9	1.0
	C5—C6	0.142	∠C12—C1—C2	120.0	C1—C2—C5—C6	0.1
	C1—C12	0.142	∠C9—C6—C7	120.0	C12—C9—C6—C7	–179.6
	C1—C2	0.142	∠C2—C5—C6	120.0	C12—C9—C6—C5	0.0

C1—C2—C5—C6 decrease and gradually reduce to zero. Interlaced planes of the reactant gradually fuse to the conjugated system, and the whole molecule becomes a nearly planar structure.

The energy relation profiles along the Cycle 1 are shown in Fig. 4. It can be seen that the maximum energy barrier correspond to TS3. So IM2→IM3 is the rate-determining step, the corresponding activation

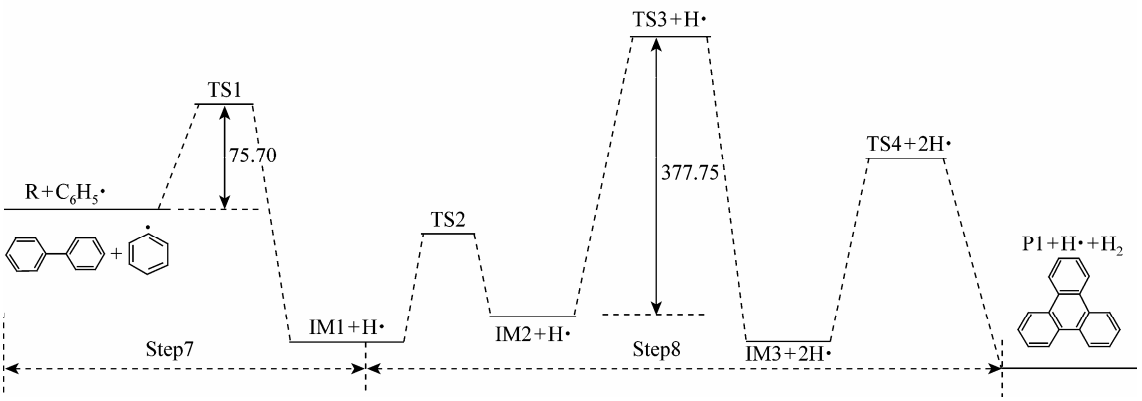

Figure 4 Energy relation profiles along the Cycle 1 in Path 2 (in kJ·mol^{-1})

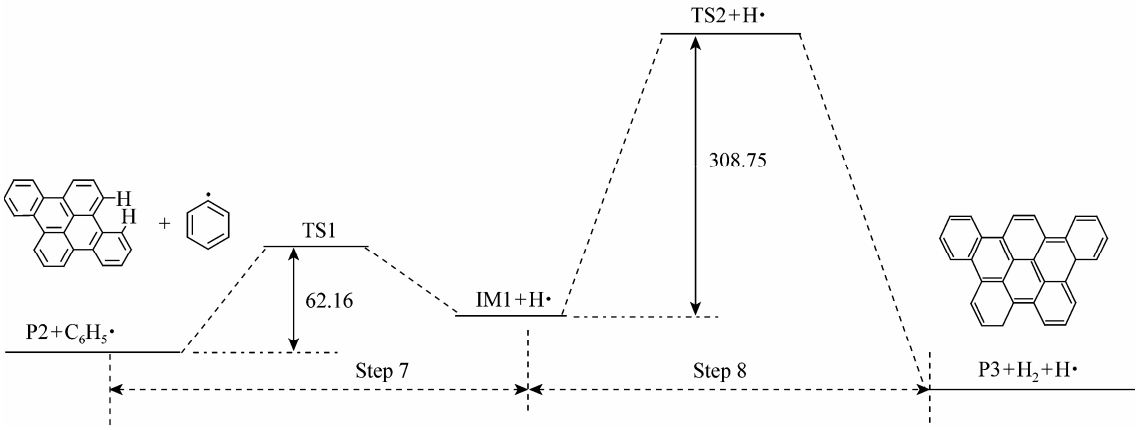

Figure 5 Energy relation profiles along the Cycle 3 in Path 2 (in kJ·mol^{-1})

energy of this cycle is 377.75 kJ·mol^{-1}. Fig. 4 shows that the energy of the reactants (R+C_6H_5·) is much higher than that of the products (P1+H·+H_2), indicating that this reaction is thermodynamically favorable. Similarly, Cycle 2 also follows the same growth process as Cycle 1, but the activation energy of Cycle 2 is 320.15 kJ·mol^{-1}.

However, by searching for the transition state in Cycle 3, we found that Step 8 underwent only one transition state. The specific kinetic calculations illustrated in Fig. 5 show that the energy of the reactants (P2+C_6H_5·) is still higher than that of the products (P3+H·+H_2), suggesting that this reaction is also thermodynamically favorable. So Step 8 is the rate-determining step of Cycle 3 in Path 2, the corresponding activation energy is 308.75 kJ·mol^{-1}. Then, Cycles 4−6 are calculated and the results show that there still exist only one transition state as in Cycle 3. Hence, it is inferred that the subsequent formation reaction of larger PCAs follows the same growth process as Cycle 3.

Interestingly, it is observed that the activation energies of Steps 7 and 8 decreases with the increasing of ring numbers of the PCAs (see Table 4). So the reaction activity of the compounds increase along with the condensation process, which could be explained by the average C—H bond length and Mulliken population of the compounds in the next section. Moreover, starting from Cycle 4, the energy barrier of Step 8 is lower than that of Step 1, Step 1 became the rate-determining step in Cycles 4−6 of Path 2, the corresponding activation energy is 307.60 kJ·mol^{-1}.

Table 4 The activation energy of every step in Path 2 with different growth cycles

Cycle	Activation energy E_a/kJ·mol^{-1}				
	Step 7	Step 8	Step 8 IM1→IM2	Step 8 IM2→IM3	Step 8 IM3→P1
1	75.70	−	96.45	377.75	254.60
2	74.35	−	98.52	320.15	232.45
3	62.16	308.75	−	−	−
4	61.76	297.96	−	−	−
5	59.75	243.97	−	−	−
6	58.69	237.24	−	−	−

3.3 Analysis and determination of the main reaction path

The activation energies of Cycles 1−6 during the growth process of the two paths are presented in Fig. 6. The main reaction path was decided by the comparison of the reaction activation energies. Because the activation energy of the rate-determining Step 3 in Path 1 is less than that of the rate-determining Step 8 in Path 2 before Cycle 4, with the increasing of ring number of fused polycyclic arenas, it is concluded that Path 1 is the main reaction path before Cycle 4, the restriction of the growth rate of PCAs is controlled by the H-elimination of benzene (Step 1). Starting from Cycle 4, Paths 1 and 2 become two-parallel reaction paths with the same rate-determining Step 1 in the whole growth process of PCAs. The growth rate of PCAs is still controlled by the elimination reaction of H atom from benzene in Step 1, and the corresponding activation energy is 307.60 kJ·mol^{-1}. It is proposed that the formation of other larger PCAs involve two-parallel Paths 1 and 2.

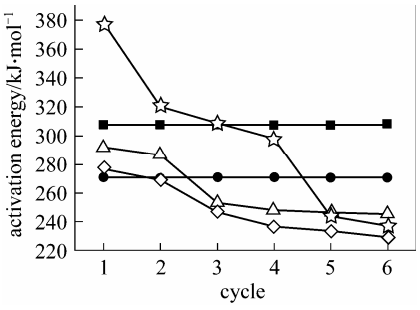

Figure 6 Activation energy profiles of different steps from Cycles 1−6 in Paths 1 and 2
■ Step 1; ● Step 3; △ Step 4; ◇ Step 5; ☆ Step 8

In addition, taking into account the average C—H bond length as well as the Mulliken population, we found that the average C—H bond length increases with the increasing of ring numbers of the fused polycyclic arenes. Correspondingly, the Mulliken population of the C—H bond decreases during the condensation process, as listed in Table 5. These results imply that the growth reaction activity increases during the process of growth reaction because of the weakening intensity of the C—H bonds, which may be induced by the delocalization of electrons on PCAs plane.

The calculation results show that the plane orientation of PCAs would be formed gradually along with the fusing of the aromatic ring. Some relevant experimental results [8, 19] validate the trends of the PCA's growth mechanism discussed above. H_2 is only the effluent gas in reaction mechanism we propose, the calculation results act in accord with the experimental facts.

Table 5 The average Mulliken population of C—H bond in the growth product of PCAs

PCA species	Molecular formula	Mulliken population of C—H bond
R	C_6H_6	0.376761
P1	$C_{18}H_{12}$	0.376455
P2	$C_{24}H_{14}$	0.375745
P3	$C_{30}H_{16}$	0.375676
P4	$C_{36}H_{18}$	0.375668
P5	$C_{42}H_{20}$	0.375424
P6	$C_{48}H_{22}$	0.375309
P7	$C_{54}H_{24}$	0.375238
P8	$C_{60}H_{26}$	0.375083
P9	$C_{78}H_{32}$	0.374995

4 CONCLUSIONS

The growth mechanisms of polycyclic arenas based on the block unit of benzene were brought forward in this study, which explained the experimental facts of no hydrocarbon species during the synthesis of carbon materials from benzene precursors. The cycle mode of two reaction paths in the growth mechanisms of polycyclic arenas and the main reaction steps of every path were confirmed. The microscopic as well as thermodynamic descriptions of transition states and intermediates in the reaction were given out, and the activation energies of every reaction step were obtained.

The growth mechanisms were applied to study the reactivity of polycyclic arenas growth; the calculation results show that the H-elimination of benzene leading to phenyl is the key step in the whole growth mechanisms of polycyclic arenas. Especially for the formation of larger polycyclic arenas, the H-elimination of benzene is the rate-determining step in the whole reaction process.

REFERENCES

1 Lai, H.J., Lin, M.C.C., Yang, M.H., Li, A.K., "Synthesis of carbon nanotubes using polycyclic aromatic hydrocarbons as carbon sources in an arc discharge", *Mater. Sci. Eng. C*, **16**, 23−26 (2001).
2 Setlur, A.A., Dai, J.Y., lauerhass, J.M., Chang, R.P.H., "Formation of filled carbon nanotubes and nanoparticles using polycyclic aromatic hydrocarbon molecules", *Carbon*, **36**, 721−723 (1998).
3 Dai, Y., Lauerhaas, J.M., Setlur, A.A., Chang, R.P.H., "Synthesis of carbon-encapsulated nanowires using policyclic aromatic hydrocarbon precursors", *Chem. Phys. Lett.*, **258**, 547−553 (1996).
4 Wang, H., Frenklach, M., "A detailed kinetic modeling study of aromatics formation in laminar premixed acetylene and ethylene flames", *Combust. Flame*, **110**, 173−221 (1997).
5 Appel, J., Bockhorn, H., Frenklach, M., "Kinetic modeling of soot formation with detailed chemistry and physics: Laminar premixed flames of C_2 hydrocarbons", *Combust. Flame*, **121**, 122−136 (2000).
6 Charles, W., Bauschlicher, Jr., Ricca, A., "Mechanisms for polycyclic aromatic hydrocarbon (PAH) growth", *Chem. Phys. Lett.*, **326**, 283−287 (2000).

7 Marinov, N.M., Pitz, W.J., Westbrook, C.K., Vincitore, A.M., Castaldi, M.J., Senkan, S.M., Melius, C.F., "Aromatic and polycyclic aromatic hydrocarbon formation in a laminar premixed n-butane flame", *Combust. Flame*, **114**, 192−213 (1998).
8 Tian, Y.J., Hu, Z., Yang, Y., Wang, X.Z., Chen, X., Wu, Q., Ji, W.J., Chen, Y., "*In situ* TA-MS study of the six-membered-ring-based growth of carbon nanotubes with benzene precursor", *J. Am. Chem. Soc*., **126**, 1180−1183 (2004).
9 Tian, Y.J., Hu, Z., Yang, Y., Chen, X., Ji, W.J., Chen, Y., "Thermal analysis-mass spectroscopy coupling as a powerful technique to study the growth of carbon nanotubes from benzene", *Chem. Phys. Lett*., **388**, 259−262 (2004).
10 Wang, B.J., Wei, X.Y., Xie, K.C., "Study on reaction of *N*-methyl-2-pyrrolidinone with carbon disulfide using density functional theory", *J. Chem. Ind. Eng*. (*China*), **55**, 569−574 (2004). (in Chinese)
11 Zheng, C.G., Liu, J., Liu, Z.H., Xu, M.H., Liu, Y.H., "Kinetic mechanism studies on reactions of mercury and oxidizing species in coal combustion", *Fuel*, **84**, 1215−1220 (2005).
12 Zhang, J.L., Wu, C.J., Li, W., Wang, Y.P., Cao, H., "DFT and MM calculation: The performance mechanism of pour point depressants study", *Fuel*, **83**, 315−326 (2004).
13 Rozanska, X., van Santer, R.A., Hutschka, F., "A DFT study of isomerization and transalkylation reactions of aromatics species catalyzed by acidic zeolites", *J. Catal*., **202**, 141−155 (2004).
14 Rozanska, X., Saintigny, X., van Santer, R.A., Hutschka, F., "A DFT study of the cracking reaction of thiophene activated by small zeolitic clusters", *J. Catal*., **200**, 79−90 (2001).
15 Violi, A., Sarofim, A.F., "Quantum mechanical study of molecular weight growth process by combination of aromatic molecules", *Combust. Flame*, **126**, 1506−1515 (2001).
16 Stewart, J.J.P., MOPAC 7.0, Quantum Chemistry Program Exchange, University of Indiana, Bloomington, IN, USA.
17 CS ChemOffice, Cambridge Science Computing Inc., Suite 61, 875 Massachusetts Avenue, Cambridge, MA02139, USA.
18 Dean, J.A., Lange's Handbook of Chemistry, 2nd edition, Science Press, Beijing (2003).
19 Hu, Z., Yang, Y., Tian, Y.J., Lü, Y.N., Wang, X.Z., Chen, Y., "High-yield production of quasi-aligned carbon nanotubes by catalytic decomposition of benzene", *Nanotechnology*, **14**, 733−737 (2003).